Artificial Intelligence and Mechanistic Modeling for Clinical Decision Making in Oncology

Sébastien Benzekry

Artificial intelligence and mechanistic modeling for clinical decision making in oncology

S. Benzekry[1,2,*]

1 : *MONC team, Inria Bordeaux Sud-Ouest, Talence, France.*

2 : *Institut de Mathématiques de Bordeaux, CNRS UMR 5251, Bordeaux University, Talence, France.*

[*] correspondence to Dr Sebastien Benzekry: sebastien.benzekry@inria.fr

The author declares no competing interest for this work.

Abstract

The amount of ‘big’ data generated in clinical oncology, whether from molecular, imaging, pharmacological or biological origin, brings novel challenges. To mine efficiently this source of information, mathematical models able to produce predictive algorithms and simulations are required, with applications for diagnosis, prognosis, drug development or prediction of the response to therapy. Such mathematical and computational constructs can be subdivided into two broad classes: biologically agnostic, statistical models using artificial intelligence techniques, and physiologically-based, mechanistic models. In this review, recent advances in the applications of such methods in clinical oncology are outlined. These include machine learning applied to big data (omics, imaging or electronic health records), pharmacometrics, quantitative systems pharmacology, tumor size kinetics, and metastasis modeling. Focus is set on studies with high potential of clinical translation, as well as applied to cancer immunotherapy. Perspectives are given in terms of combinations of the two approaches: ‘mechanistic learning’.

Introduction

Cancer diseases are a major health concern in the modern society. Taken together, they were responsible for 9.6 million deaths in 2018, which represents nearly 1 in 6 deaths [1]. In face of such a public health challenge and considering the "unreasonable effectiveness of mathematics in natural sciences" [2], one might wonder: can mathematical models be of help in oncology?

Mathematical constructs have long been confined to the representation, understanding and prediction of physical systems. The first reported use of a mathematical model in the life sciences is an epidemiological model by D. Bernoulli in 1760 who aimed to study the impact of "vaccination" (inoculation of a small amount of the disease) against smallpox on age distributions and life expectancy [3]. His calculations predicted that "vaccination" would result in a net life expectancy gain of 3 years.

With the modern development of novel measurement methods (especially from molecular biology and imaging), accumulation of biological and clinical data is currently driving oncology towards a quantitative science, which raises the challenge of inferring general patterns and structures as well as extracting most information from these. Meanwhile, the number of mathematical models developed by theoreticians in the field of so-called "mathematical oncology" [4] has been exponentially growing in the last decades [5,6]. However, these formal constructs have often remained confined to qualitative conclusions and rarely been confronted to observations. Two possible aims can be conceived for mathematical modeling in oncology:

- better understand. By allowing the simulation (or analysis) of the implications of biological hypotheses, mathematical and computational models provide a way to test them against experimental data. This improves our understanding of the biology by discriminating theories that are able to describe the data and, perhaps more importantly, reject theories that are not.

- better predict. In this case, even if the model is biologically-agnostic (relying on no *a priori* biological knowledge), if its predictive power is properly validated, it can provide a powerful numerical tool for clinical applications. These can be divided into: (a) diagnosis, (b) prognosis/prediction of response, (c) drug development and (d) personalized medicine (see examples in Tables 1 and 2).

In this review, we will only deal with models with the second aim. Such models can be broadly divided into two categories: artificial intelligence and mechanistic models (Figure 1). The first category implements biologically-agnostic statistical learning algorithms while the second deals with the modeling and simulation of actual physiological processes, in order to make predictions in a second phase.

Artificial intelligence for clinical oncology

Artificial intelligence (AI) is a sub-discipline of computer sciences that aims at reproducing, by means of algorithms (implemented in computers, i.e., machines), processes that usually require human intelligence (e.g. vision or language). A sub-branch of AI, termed machine learning (ML), refers to those algorithms that are largely built from data, in opposition to being explicitly programmed according to a set of predefined, static, rules. ML is an extension of traditional statistical techniques, with varying degree of human intervention along a continuous spectrum. ML algorithms relevant to clinical application can be divided into unsupervised and supervised learning. Unsupervised learning deals with the process of finding patterns from a given set of input data only (e.g., define a relevant classification of cancer from molecular expression data), while supervised learning tries to predict outcomes (e.g., benign versus malignant) from the input data (e.g., lesion images). It does so by learning the relationships between input and output from training sets, with the hope of being generalizable to other data unseen before. Classical approaches of ML comprise linear and logistic regression, decision trees, random forests, support vector machines and artificial neural networks, among others [7]. In several instances relevant to clinical oncology, outputs to be predicted are time-to-event – thus censored – data, e.g. disease-free, progression-free or overall survival (OS). Consequently, these require adaptation of the ML algorithms for handling censoring. To deal with high-dimensional data, LASSO (i.e., L^1 penalization) or ridge (L^2 penalization) have been combined with classical Cox regression [8]. In the past few years, the field of machine learning has seen dramatic advances driven by impressive successes of deep learning (DL) [9,10]. DL algorithms are artificial neural networks with multiple hidden layers. In a given layer, the output of a neuron is made of the composition of a linear map of the outputs from the previous layer, and a nonlinear activation function (e.g., sigmoid). This nonlinear structure allows DL to capture complex mathematical relationships between the

input data and the output. DL models can have millions of parameters and thus require massive amounts of data to be trained. The advent of 'big data' in contemporary years, combined with the increase and accessibility of computing power, has unleashed powerful applications of DL [10]. In clinical oncology, such 'big data' come primarily from three sources: omics, images and electronic health records.

Omics data

Empowered by the public availability of large-scale, multi-omics cancer databases (e.g. The Cancer Genome Atlas (TCGA, https://www.cancer.gov/tcga) or Gene Expression Omnibus (GEO) [11]), ML analyses have the potential to drive omics-based precision medicine. The first ML studies implemented classification tasks. Given high-throughput molecular data (e.g., gene expression), ML methods have been applied to distinguish between myeloid and lymphoblastic acute leukemia [12], determine cancer type [13], establish a molecular classification of breast cancers [14] or define gene expression signatures predictive of survival or metastatic relapse, for instance in breast [15], lung [16], colorectal [17] or central nervous system [18] cancers. This was achieved using methods from unsupervised learning such as hierarchical clustering [19], principal component analysis (PCA)-based clustering [20], k-means clustering or, more recently, t-distributed Stochastic Neighbor Embedding (t-SNE) [21].

For tasks such as personal prediction of outcome (e.g., survival, or metastasis-free survival) from a patient's molecular profile, supervised learning has been employed, first using traditional ML techniques [7]. For instance, Listgarten et al. found that a support vector machines algorithm performed best at predicting breast cancer presence from single nucleotide polymorphisms data [22]. Then, fueled by the success of deep learning in handling high dimensional data, recent studies have applied deep artificial neural networks with omics data as input [23]. For instance, Ching et al. proposed Cox-nnet, an artificial neural network for

prediction of survival from transcriptomic data [24]. The model is composed of two layers: one hidden, fully connected layer and one Cox regression layer. The model was found to exhibit same or better predictive accuracy compared to Cox-LASSO, Cox-ridge, or random survival forests. Other examples include survival prognosis from multi-omics data in hepatocellular carcinoma [25], breast cancer [26], or multiple data sets from the TCGA [27]. In order to deal with the "curse of dimensionality" inherent to the very high number of features (consider that gene expression data can span approximately 20,000 genes), investigators have implemented various feature selection strategies to reduce dimensionality [26], including using neural networks themselves [24]. Of note, DL methods have been shown able to integrate multi-omics data spanning RNA and miRNA sequencing, methylation data and copy number alterations [25,26].

Imaging data

AI is arguably most proficient in leveraging high-dimensional data provided by images (high number of pixels/voxels). This is due to the successful application of a particular type of DL termed convolutional neural networks (CNN) to computer vision tasks. One emblematic success of AI in oncology in recent years has been to reach dermatologist-level performances for classification of skin cancer and diagnosis of melanoma from a photograph of the lesion [28]. However, the two main sources of images in clinical oncology are from digital pathology and radiological images.

Digital pathology

Applied to digital pathology slides, CNNs have been able to reach great success for the detection of the presence of lymph node metastases in breast cancer, with area under the roc curve (AUC) as high as 0.996 in an external validation set and a sensitivity of 91% at 1 false-positive per patient [29]. Going further, such work led to the development of an augmented-reality microscope with real-time indication of susceptible areas [30]. Pushing the concept and using DL to “see” better in digital pathology, Kather et al. trained a CNN to classify the stromal

components (such as lymphocytes, adipose tissue, smooth muscle, etc.) in colorectal cancer histopathological slides, using 100,000 image patches [31]. The CNN showed excellent accuracy (99% on training, 94% on test set) and formed the basis of a "deep stroma score" (combination of mean activations of the output neurons defining the classes (i.e., tissue type)) that showed prognostic significance for OS and relapse-free survival, both in Cox univariate analysis and multivariate analysis with classical factors. The same authors further showed that DL could predict microsatellite instability (a critical predictive biomarker of response to immunotherapy) from hematoxylin and eosin histology in gastrointestinal cancer [32], a finding similar to another study where a DL algorithm was used for classification of lung cancer histological subtypes [33]. Others also used DL for prediction of survival from histology in malignant mesothelioma and found a critical role of the stroma [34], similar to Kather and colleagues [31].

AI for diagnosis and segmentation from radiological images

Another important source of high-dimensional data to feed AI algorithms is provided by radiological images, including radiography, computed tomography (CT), magnetic resonance imaging (MRI) and functional imaging (e.g. positron emission tomography (PET)). These can be used either for diagnosis (i.e., detecting the presence of a cancer), automatic segmentation (delineation of a tumor in an image) or prognosis/predictive (e.g., predicting response to therapy) purpose. In breast cancer, following the generalization of mammography screening, an important challenge is to be able to detect the presence of cancer lesions in the images. This task usually requires trained experts and can be time-consuming. To address this issue, recent advances have been made whereby AI systems (deep CNNs) have been shown able of superior predictive power than human experts, in large (>20,000 subjects) databases [35,36]. Similar results have been obtained for reducing false positive and false negative rates in lung cancer screening, with an area under the ROC curve of 0.944 [37].

For segmentation tasks, multiple studies used a technique called transfer learning, that is, the adaptation to their purpose of a previously developed CNN for another (computer vision) task [38]. For instance, the U-Net model architecture, initially developed for segmentation of neuronal structures from microscopy images, has been successfully applied to the segmentation of pulmonary nodules from CT [39], or the segmentation of liver metastases from colon cancer [40]. Other methods – still relying on deep CNNs – have been used for the segmentation of brain tumors from MRI [41].

Radiomics

Fueled by the availability of open source libraries such as PyRadiomics [42] and free software [43], the number of studies relying on radiological images as a source of data and applying computational medical imaging (radiomics) methods has been growing exponentially in recent years, since the introduction of the term 'radiomics' in 2012 [44]. In such works, quantitative features are computed from the images to serve as biomarkers. These can either be handcrafted – i.e. metrics related to the shape, intensity or heterogeneity of some region of interest –, or automatically extracted from the image, for instance from some layers of an artificial neural network [45]. Several radiomics studies have been conducted in lung cancer by the group of Aerts for either prediction of distant metastasis [46], genetic mutations (*EGFR* and *KRAS*) [47] or gene expression profiles [48]. In sarcomas, Crombé et al. have established a delta-radiomics (i.e. difference of radiomic features between two time points) signature for prediction of response to neo-adjuvant chemotherapy [49].

The first radiomic study for prediction of response to immunotherapy was provided by Sun et al. [50]. Using radiomic features from both the tumor center and peripheral area, in combination with clinical features, the authors developed a signature on an internal dataset and validated it in 3 external cohorts: 1) a TCGA dataset, which confirmed association of the radiomics signature and RNA-seq based quantification of CD8 T cells infiltration, 2) a histology dataset

with direct assessment of immune infiltration and 3) a third dataset with phase I patients treated with immunotherapy (for predictive value). However, a closer examination of the results reveals that most of the predictive power was driven by non-radiomics variables (e.g. tumor location, or imaging machine setup) and not by the radiomics features themselves [50]. Similar observations have been made whereby radiomics signature has been found not to contain much additional value than the mere tumor volume [51]. Thus the added value of radiomics should always be adjusted for possible confounding factors included in simpler variables.

A few radiomics studies have been published using DL and radiological images for prognosis or prediction of response to therapy. In these, DL models are applied directly on the images without pre-engineering of the image into well-defined features, as done in classical radiomics approaches. This allows an easier application of the algorithms, since it does not require fastidious segmentation of the area of interest. In addition, the AI analyzes the entire image which might contain informative patterns rather than the tumor itself (e.g. surrounding tumor stroma). Applications include prediction of disease-free or overall survival in nasopharyngeal cancer [52] from PET/CT images, in non-small cell lung carcinoma (NSCLC) from CT images [53], and in glioblastoma from MRI [54]. The models are often used to derive a large number of DL-based features, subsequently plugged into a LASSO-Cox proportional hazard model. Interestingly, in contrast to several reports of the superiority of DL in imaging in general [45], in several comparative studies in oncology, investigators found no difference between DL and classical radiomics [55,56]. For the highly agnostic DL models, using a single image – especially from non-functional, anatomical imaging such as CT-scans – can have limited prognosis value [57]. In such cases, exploiting the information contained in longitudinal images can bring added value [57].

Electronic health records

Even though yielding promising results, the applications of AI mentioned above have not yet reached the maturity to be transposed to the clinic, and only a handful of AI algorithms have been approved by the American food and drug administration [10]. Meanwhile, the digitalization of health records also provides a source of massive, mineable data. Probably the most clinically advanced tool in the analysis of such data is IBM's cognitive decision-support system, Watson for health. Relying heavily on literature data (processed automatically using natural language processing) and expert knowledge (mostly from oncologists at the Memorial Sloan Kettering Cancer Center), IBM's tool aims at providing guidance in individualized treatment decisions. Although no prospective, randomized clinical study has been reported yet, IBM Watson has been deployed in multiple clinical institutions over the world. Testing concordance with actual clinical decisions, results have been contrasted, some reporting high concordance (93%) in breast cancer [58], while others found a low concordance (48.9%) in colon cancer [59]. Overall, application of Watson has led to disappointing results so far, in terms of individual treatment planning with existing strategies as well as with potentially innovative treatments [60]. Explanations have been proposed in that it mostly reflects the decisions of the experts who trained it [60].

Mechanistic modeling

As seen above, AI has been very proficient at mining high-throughput data. In particular, the most impressive successes have been in imaging. This can be interpreted as a consequence of the actual structure of DL models, which mimicks actual neurons in the brain, directly involved in tasks such as vision. However, despite this “physiologically-inspired” structure, AI algorithms suffer multiple limitations such as their lack of interpretability [45] or the requirement of very large annotated and properly curated data sets. Moreover, AI algorithms have so far been able to reach human performances but rarely outperformed them. For other tasks than vision such as clinical decision making and therapeutic management (e.g., predict the impact of a given change of dose or scheduling of a drug), AI has yet to demonstrate its applicability. Limitations in terms of interpretability of AI algorithms calls for incorporation of biological knowledge into the models, also called “visible” machine learning [61]. In contrast to biologically-agnostic AI models, mechanistic approaches develop physiologically relevant models able not only to link input and output, but also to simulate the kinetics of oncogenic processes and treatment (Figure 1). They are thus linked to the type of relevant data amenable to quantification. The main categories of such data are pharmacological data (e.g., plasma drug concentrations) and tumor size (from radiological techniques). Figure 2 recapitulates the classes of mechanistic models relevant to oncology. In recent years, cancer research and clinical oncology have focused on cancer immunotherapy, in particular with the advent of immune-checkpoint inhibitors (ICI) [62]. Consequently, mathematical modeling studies have addressed relevant issues relating to immune-oncology drug development or for clinical care.

Modeling in (immune-)onco-pharmacology

Pharmacometrics

Historically, population pharmacokinetics (PK) modeling has been initiated by the pioneering work of L. Sheiner in the 1970's [63]. The aim of such quantitative approach is twofold. First, to translate the actual PK physiological processes into simplified, abstract mathematical constructs (the structural model, e.g. a compartmental model). Second, to capture inter-individual variability into statistical distributions of the parameters of the structural model, and to quantify the impact of covariates on such physiologically-inspired parameters (e.g. clearance or volume of distribution). Individual predictions from sparse data can further be obtained using empirical Bayesian estimation.

Population PK studies for ICI (monoclonal antibodies) have been performed over the last 6 years and have found that two-compartmental models were often appropriate for description of the concentration time course of these drugs. They have revealed large inter-individual variability and low, possibly time-varying [64–66], clearance. Studies have been conducted for ipilimumab [67], nivolumab (alone [64] or in combination with ipilimumab [68]), pembrolizumab [69], atezolizumab [70] and durvalumab [71], in multiple tumor types. These studies allowed simulation of varying dosing regimens, and were generally supportive of similar PK exposures between weight-based and flat-dosing regimens. Nevertheless, due to the large inter-individual variability, the use of therapeutic drug monitoring to personally adapt the dose of monoclonal antibodies has been proposed, although not clinically applied so far [72].

Downstream the dose-concentration-exposure relationship, exposure-response (ER) studies aim at quantifying the dependency of efficacy (e.g., overall survival) on exposure metrics (e.g., AUC), see Figure 2. As with other monoclonal antibodies used in oncology, the ER relationship is complex, in particular due to 1) confounding baseline factors on clearance (better prognostic associated with lower clearance) and 2) for ICI at least, time-dependent

clearance due to variable clearance with disease status [65,66]. Adjustment to baseline prognostic in ER models is needed (to address 1) and use of early exposure metrics (first cycle) is for now the best approach to mitigate for 2) [65]. ER modeling has been performed for ipilimumab [73], nivolumab [74,75], pembrolizumab [76] or atezolizumab [77]. For example, Feng et al. [75] used several model-derived individual PK parameters (e.g. the average drug concentration during the first cycle, to mitigate for 2) as measures of exposure and a multivariate Cox model (to adjust for 1) to relate them to OS. Overall response and adverse events were modeled using logistic regression. Baseline clearance was a proxy for unobserved baseline prognostic factors (e.g., disease status). They concluded that the ER relationship for nivolumab was flat (a conclusion shared with others [74,77]), which further supported the subsequent label change for nivolumab from 3 mg/kg Q2W to flat dosing, first 240 mg Q2W and then 480 mg Q4W based only on *in silico* simulations [78]. However, as stated above the ER relationship for ICI and further mechanistic modeling warranted to address, e.g. the circular relationship between clearance and disease status/cachexia [75,76].

Quantitative systems pharmacology in immunotherapy

Quantitative systems pharmacology (QSP) studies in oncology investigate the complex mechanisms of action of anti-cancer agents, in order to determine, for instance, safe and effective doses for first-in-human studies [79]. Such QSP study of the PK/pharmacodynamics (PD) of pembrolizumab was performed by Lindauer et al. [80]. The authors combined compartmental PK for systemic distribution of the drug, physiologically-based (PB) PK for tumor-site distribution, a model of binding of pembrolizumab to its target PD1 and a tumor growth inhibition model for efficacy of anti-cancer agents in experimental systems (without the transit compartments that were found insignificant). The model was developed to predict the minimally effective dose maximizing the probability of at least 30% growth reduction. Validation was conducted in animals with several doses and measurements of receptor occupancy in the blood and at the tumor.

Translation to human was performed leveraging the PBPK components as well as replacing the compartmental PK module by a human one and using allometric scaling for some remaining PD parameters. The results suggested 2 mg/kg Q3W as the minimal dose, with no further improvements in the range 2-10 mg/kg. Interestingly, this flatness of the dose-response relationship was confirmed in the modeling analysis of the clinical studies [81]. Optimal dosing of another anti-cancer agent using an immunocytokine was investigated by Ribba et al. [82]. Since their drug is able to bind to immune cells, the authors had to develop an advanced target-mediated drug disposition mathematical model, which they used to predict tumor uptake retrieved from imaging data. They found that a dose-dense schedule could improve the biodistribution of the drug and showed how their model could be used to individualize treatment plans.

Despite the important success of ICI treatments, long-term efficacy is only limited to a minority of patients [83]. Therefore, combining ICI with other therapeutic modalities is an appealing strategy to harness anti-tumor immunity. In an elegant study, Palmer et al. demonstrated that in several cases of drug combinations (including ICI combinations), the population-level benefit over monotherapies observed in clinical trials could be explained by the concept of drug independence whereby there is no actual synergy or additivity at the individual-level but rather population-level superiority solely due to individual patients responding to the drugs they are most responsive to, with no added benefits from other drugs [84] 3. Meanwhile, mechanistic modeling could play an important role in determining the best modes of combination between ICI and established treatments (surgery, radiotherapy, chemotherapy, targeted therapy) [85,86]. Modeling immunotherapy has recently been stretched to gain insights on optimal modalities for combinations with radiotherapy (RT) [87,88]. Based on the rationale that local radiotherapy increases systemic activation of the immune system through the release of neo-antigens – the ‘abscopal effect’ – these studies have translated the cancer-immune interplay into mathematical constructs to predict the impact of different therapeutic schemes. Based on a

thorough understanding of immunological mechanisms, Kosinsky et al. used multiple experimental groups (of a murine colon carcinoma model), spanning different combination schedules, for development and validation of a detailed QSP model incorporating radiotherapy and anti-PD(L)1 therapies [88]. It included multiple processes such as immunogenic cell death and dendritic cell maturation, time course of PDL1 expression and Treg:CD8+ ratio. Despite its complexity, the model parameters were either found in the literature or identifiable from fitting the experimental data, and validation was carefully conducted in independent datasets. The model gave interesting insights about responders and non-responders, classified so from the only source of inter-animal variability in the model, a parameter responsible for T cell infiltration into the tumor tissue. Simulation of various alternative combination regimens were conducted and suggested that optimal efficacy was obtained when anti-PD1 treatment was administered prior, or concomitant to the radiotherapy, using hypo-fractionated schemes. Such predictions could have value to guide clinical trials among a vast range of combination possibilities. Others proposed a simple model calculating an 'immunologically effective dose (IED)' proposed for radiotherapy fractionation schemes [89]. Relying only on two additional parameters to the classical α and β of radiobiology – two physiological time constants that were derived from the literature – the model could reproduce preclinical data and gives a valuable tool for *in silico* exploration of immunogenicity of RT regimens (see online calculator www.smartcalculators.online/ied). For instance, the scheduling used in the PACIFIC study [90] (i.e., 5x2 Gy for 6 weeks) was predicted to have only modest IED efficacy (12%), whereas another scheduling with same biologically equivalent dose would increase IED efficacy (i.e., 74% with 3x8 Gy for 6 weeks). This suggests that algorithmic strategies could lead to higher immunogenicity and achieve synergism between RT and ICI.

More generally, the question of the optimal combination between different anti-cancer agents with different modes of action is well-adapted for mathematical

modeling [85]. For instance, several studies have investigated the combination of anti-angiogenics with chemotherapy [91,92]. The biological rationale is that anti-angiogenic agents such as bevacizumab induce a transient amelioration of the tortuous and poorly functional blood vessel network of a tumor, in a process called vascular normalization. In turn, this could improve the delivery of chemotherapy, which is always administered in combination with bevacizumab. Whereas clinical use is to give both drugs concomitantly, these observations suggest possible value to sequential administration, but an open question remains the optimal time interval between the two administrations. Imbs et al. used a first set of experiments to calibrate a model for this synergistic effect, and then demonstrated that the model predictions – an optimal time interval of 3 days between administration of bevacizumab and the chemotherapy doublet pemetrexed-cisplatin – were concordant with a second, validation experiment [92].

Design of early-phase clinical trials

Historical concepts

Historically, several concepts of clinical and pharmacological oncology have been developed in connection with mathematical models [93]. For instance, the Maximum Tolerated Dose (MTD) paradigm emerged following the work of Skipper, Schabel and Wilcox in the 1960s [94]. Working on leukemic cell lines, they observed exponential growth of the cell populations. In addition, they found that given concentrations of cytotoxic drugs (including 6-mercaptopurine, 5-fluoruracil and vinblastine), instead of killing given amount of cells, were killing a constant *fraction* of cells, the so-called *log-kill* effect [94]. This pharmacodynamic relationship between exposure and effect was further substantiated by Jusko [95] based on the premise of an irreversible reaction between the drug and the cells receptors, and possibly accounting for two cell subpopulations (sensitive and resistant) [96]. Following the further realization that the presence of as little as one single leukemic cell was sufficient to lead to the host death, they argued that the

goal of the therapy should be to achieve complete cure of the disease, i.e. eradication of all malignant cells. In this context, they demonstrated that a large-dose/short time (single administration) schedule was superior to a chronic (daily) low-dose schedule (with similar or larger total dose).

Later, Norton and Simon revised both the growth model and, consequently, the action of chemotherapy on tumor kinetics [97]. Arguing that for solid tumors (e.g., breast), there is a mechanical stress constraining growth, they favored a model of tumor growth exhibiting slowdown, for instance the Gompertz model [98]. Going further, since this consideration suggested a non-constant fraction of proliferative cells in the tumor, and considering that chemotherapy action is mostly based on anti-mitotic agents, they proposed and validated the Norton-Simon hypothesis, which consists in applying the killing term only to the actively proliferating fraction. Importantly, this theoretical concept suggested that densified regimen would achieve higher probability of cure, an idea that was further successfully tested clinically for adjuvant therapy in breast cancer [99].

Recent studies

Beyond the classical MTD paradigm, mathematical models have started to be applied to help the design of early-phase clinical trials. The first concern in such trials is safety, in particular controlling life-threatening hematological toxicities in the context of aggressive regimen such as the dose-dense schedules mentioned above. In this context, an opportunity for mechanistic modeling is given by the fact that dynamics of neutrophil counts and myelosuppression can be quantified [100]. To control severe neutropenia and make dose-dense regimen clinically safe, Meille et al. developed a combined PK-PD model incorporating both efficacy and toxicity [101]. This model was clinically applied in the MODEL1 trial (NCT02392845), to optimize the administration of a combinatorial regimen of docetaxel and epirubicin in breast cancer [102]. The algorithm was used to find the repartition of the two drugs during the densification process (from three to two weeks) that would ensure minimal tumor size while respecting toxicity

constraints. Resulting from the optimization was a non-trivial schedule, which was also possible to be adapted individually, using measurements from the first cycle(s) and empirical Bayesian estimation. This study resulted in a successful densification of the protocol, with much lower hematological toxicity and higher efficacy than reported in other studies with standard dosing [102]. A similar strategy – although with a different underlying structural model – was employed to design the MetroVino trial (NCT02555007) for administration of metronomic vinorelbine in lung cancer [5,103]. However, it remains unclear how to articulate the relative benefits of dose intensification and metronomic administration.

The previous models did not account for relapse/resistance to therapy, a phenomenon widely observed in the treatment of advanced cancers. This is due to intra- (and inter-) tumor clonal heterogeneity [104]. A tumor is composed of multiple clones with varying degrees of sensitivity to a given drug, either pre-existing at the beginning of therapy or emerging during the course of treatment, which is only effective against the sensitive cells. It is thus a tempting avenue to hypothesize that different dosing regimens impact differently on the appearance of resistance. In particular, the classical MTD paradigm might not be best adapted since it might lead to eradication of all sensitive cells, thus leaving space and nutrients available for resistant clones. This eco-evolutionary view of tumor growth has led several investigators to design mathematical models aiming at controlling resistance phenomena, from early studies by Goldie and Coldman [105] to more recent works by Michor [106,107] or Gatenby [108]. The Michor group for instance has transposed biological principles of cancer evolutionary dynamics into mathematical models relying on stochastic processes to understand and predict the onset of resistance to anti-EGFR therapies in lung cancer [109]. Using models of polyclonal tumor growth in which each cell can randomly divide (with or without mutation), live or die, and preclinical data to calibrate their model, an alternative dosing strategy for erlotinib in the treatment of EGFR-positive patients with NSCLC was proposed [106]. The strategy was based on a combination of pulse dose twice weekly and daily low-dose. It was

further tested in a phase I clinical trial where it unfortunately did not outperform the standard scheme, but nevertheless was well tolerated and prevented progression of central nervous system metastases [107]. Although basic PK modeling was considered, no extensive pharmacometrics (incorporating mixed-effects statistical learning) was included. This feature could have helped control variability in peak serum concentrations, which was proposed by the authors as a likely explanation of the modest results obtained [107].

Using similar eco-evolutionary principles for tumor heterogeneity, the concept of 'adaptive therapy' was proposed by Gatenby [110]. Arguing that sensitive cells compete with resistant cells within the tumor, it suggests to treat only upon progression, on a patient-by-patient basis. After confirmation of the superiority of this strategy over classical MTD or metronomic schedules in animal experiments [111], 'adaptive therapy' was successfully transposed at the bedside in metastatic castrate-resistant prostate cancer patients [112].

Tumor size kinetics

Tumor growth inhibition modeling

The generalization of computerized tomography for imaging tumor lesions allows to collect, non-invasively, quantitative measurements of lesions sizes at multiple time points. These radiologic measures are employed to evaluate response to therapy during follow-up by means of the Response Evaluation Criteria In Solid Tumors (RECIST) [113], used nowadays to make go/no-go decisions at the end of phase II trials. RECIST consists in following target lesions defined at baseline, and computing variations of the sum of their largest diameters to categorize response (progression, stable disease, complete or partial response). By doing so, longitudinal and continuous information about the response to treatment is lost. Consequently, RECIST-derived metrics such as overall response rate (ORR) and progression-free survival (PFS) are only modest surrogates of the gold standard for evaluating efficacy of a treatment, i.e. OS. Indeed, OS results can differ, even though PFS and ORR are not

different (e.g., between 3 mg/kg and 10 mg/kg for ipilimumab [114]). Therefore, strategies aiming at modeling the full time course of response are appealing, and might provide better predictors of OS. Such tumor kinetics models (also called tumor growth inhibition – TGI – models) have now been widely used since their initial introduction by Tham et al. [115], Wang et al. [116], Claret et al. [117] and Stein et al. [118]. They are often coupled to parametric or semi-parametric proportional hazard survival models for description and prediction of OS from model-derived covariates [116,117].

While TGI modeling is now more than a decade-old [119], with models of increasing complexity to describe advanced growth processes related to, e.g., prolonged response from chemotherapy or radiotherapy in gliomas [120], recent works have focused on applying the methodology to data from clinical trials involving ICI. Patterns of response to immunotherapy may often differ from those observed with more classical anti-cancer agents. Response to ICI may exhibit long term stabilization of disease or response, or conversely different patterns of progression (i.e. pseudo/hyper-progression). Although this can be tackled using more complex models, e.g. with second-order kinetics [121], biphasic zero/first-order kinetics models have been successfully adapted to the ICI context [81,114,122–124].

TGI modeling for immunotherapy

To address the heterogeneity of response patterns to ICI, mixture models – whereby some parameters are considered to depend on a latent variable defining multiple classes – have been considered, for instance for pembrolizumab [81] and ipilimumab [114], in advanced melanoma. This approach allows to account for multiple groups (e.g. fast, intermediate and no growth). Going further, Chatterjee et al. also proposed a single model with no mixture component that was able to describe the entire population [81]. The model is an extension of the Stein biexponential model [118] and writes:

$$S(t) = S_{baseline}\left((1-f)e^{k_{growth}\cdot t} + fe^{-k_{death}\cdot \max(0,t-delay)}\right), \qquad (1)$$

where f is a parameter controlling the fraction affected by the shrinking effect and $delay$ is a time lag allowing to describe delayed response. The link with exposure was provided by a dependence of the parameter k_{death} on the individual area under the concentration curve. Contrasting implications about the dosing of ICI antibodies have been obtained from these dose/exposure-response models. While Chatterjee et al. concluded to no difference between 1 mg/kg and 10 mg/kg Q3W [81], Feng et al. found that the dose was associated with the mixture subpopulation, thus the response [114].

Analyzing trial data of atezolizumab compared to docetaxel in the treatment of NSCLC, Claret et al. demonstrated the applicability of TGI models to forecast the outcome of phase III trials [122]. Using only data from a phase II trial for calibration of their TGI-OS model (a sum of two exponentials, $S(t) = e^{-dt} + e^{gt} - 1$ similar to [118], linked to a lognormal survival model), they identified the growth rate g as a highly significant covariate of OS and were able to predict the results (hazard ratios) of an independent phase III study, from the data of the size kinetics. They also demonstrated that such prediction could be achieved as soon as 40 weeks after study initiation, which corresponded to 30 weeks before what could be concluded from the observed data only. In addition, their analysis underscores the added value of TGI-OS models compared to RECIST alone, because the significant OS difference between the two arms was not detectable in ORR or PFS only.

In the context of complex tumor-immune interactions, tumor size is not the only relevant longitudinal biomarker of response to therapy. With the development of immune-monitoring techniques, cellular and molecular players are amenable to quantification and it is thus appealing to design more advanced mechanistic models. In the first such study, Netterberg et al. selected interleukin (IL) 18 as having the most significant variation among 95 plasma biomarkers initially

considered [123]. They further built a mechanistic model integrating 1) PK of the drug (atezolizumab), 2) kinetics of IL18 (indirect response model) and 3) tumor size kinetics (similar to Claret et al. [117] but with a zero order growth term). Their analysis unraveled the effects of exposure (area under the curve) on the magnitude of the response and those of relative change in IL18 on response duration, emphasizing the utility of immune-monitoring to predict response. However, a subsequent study demonstrated that IL18 had no significant impact on OS [125].

Joint models

TGI-OS models estimate the TGI and OS model parameters sequentially. This can be prone to bias because the survival time can be informative of the tumor kinetics (patients relapsing fast have a more aggressive disease) [126]. On the other hand, joint models propose to estimate simultaneously the parameters of the entire model, by defining and maximizing the likelihood of the full data set (longitudinal measurements + survival) in a single step. This joint modeling approach has recently flourished in oncology to analyze tumor size (or biomarker) kinetics and overall or disease-free survival [124,127,128]. Tardivon et al. developed the first model of this kind for cancer immunotherapy (atezolizumab in urothelial carcinoma) [124]. Using a similar model as equation (1) for tumor size kinetics, the authors identified two model-derived metrics as significantly associated with OS (time to growth and current SLD slope). Importantly, their model demonstrated good predictive ability of individual death times in an external validation data set, with time-dependent areas under the ROC curve all above 0.75, significantly higher than when the kinetic model metrics were not included in the model. Król et al. added an important supplemental layer to joint modeling of size kinetics and survival: the appearance of non-target lesion (recurrent event) [127]. This event is indeed a criterion for progression in the RECIST criteria and has an impact on survival, which is neglected in classical TGI-OS models. Using a link between the two types of time-to-event-data

(=frailty), the authors demonstrated the utility of this approach to individually predict probability of death from on-treatment data.

Modeling metastasis

Inter-lesion heterogeneity

The vast majority of tumor size kinetics models describe the main quantitative output underlying RECIST: the sum of largest diameters of target lesions. However, modeling this sum as a single mass prevents a truly mechanistic modeling of the disease growth, because the actual processes happen at the tumor level. As soon as the model is nonlinear, kinetics of the sum differ from the sum of the kinetics (e.g. the sum of two exponentials with different rates is not an exponential). Moreover, interactions between established tumors – a phenomenon termed 'concomitant resistance' – might blur the picture when modeling the total cancer burden [129]. Therefore, the question of modeling inter-lesion variability (ILV) within the same host is of important relevance and has started to attract the attention of mathematical modelers in recent years [130–133]. In a model including a hierarchical layer for ILV for the kinetics of standard uptake values (SUV) from positron emission tomography (PET) imaging in sunitinib-treated gastrointestinal stromal tumors, Schindler et al. found a significant ILV for the drug effect, although smaller than inter-patient variability [134]. This finding was also observed in another study modeling ILV and comparing the OS predictive power of model metrics (time-to-growth) derived from either diameters or volumes (computed from semi-automated tumor segmentation) in 918 metastatic colorectal cancer patients [130]. Inter-lesion heterogeneity was further analyzed by Mistry et al., by means of mechanistic models of resistance (either *de novo* or acquired), leveraging multiple phase III trial data [131].

Dynamics of metastastic birth

A cancer disease is not limited to growth processes. In the context of a population of multiple tumor lesions, the appearance of new tumors is a crucial

step. While this process can be modeled using joint modeling as mentioned above [127], mechanistic approaches have also been proposed [135–137]. These could address a critical clinical challenge for cancers diagnosed at early stages: who should receive adjuvant therapy in addition to surgery, and how much?

In a landmark paper, Iwata et al. proposed a structured partial differential equation model for the size distribution of regional metastases from an hepatocellular carcinoma [135]. Using a Gompertz growth law and a dissemination rate proportional to the tumor surface (i.e. $V^{2/3}$ if V is the tumor volume), they were able to accurately describe clinical data of visible metastases in one patient. Critically, their model is able to make inference about the number and size of invisible metastases, from the observations of the visible ones only. It has been further validated using mixed-effect techniques for inter-animal variability in nonsurgical [138] and surgical [139] animal models of metastasis. In the latter, the model was simplified: secondary metastases (metastases from metastases) were neglected and the dissemination rate was assumed to be proportional to the tumor volume. The model was also able to fit the probability of metastatic relapse as a function of primary tumor size in 2,648 breast cancer patients, with inter-patient variability captured in the statistical distribution of only one parameter [139]. Similar metastatic modeling was applied to clinical data of brain metastases in NSCLC [137], where it suggested periods of dormancy of the order of 5 months and demonstrated how prediction of metastasis could help to guide clinical decision for whole brain radiation therapy (Figure 3).

Mathematical modeling has also been used to shed light on a neglected, but nevertheless critical aspect of metastatic dynamics: post-surgery metastatic acceleration. Analyzing the patterns of relapse hazards following breast cancer surgery, Retsky et al. noticed a bimodal distribution that could be explained using a computational model incorporating surgery-driven acceleration [140]. Growth suppression by the primary tumor – subsequently leading to post-surgery acceleration – was also mathematically inferred in another study by

Hanin et al. analyzing data of 55 lung metastases from a kidney cancer patient [141].

Metastatic appearance and growth has also been studied through the lens of clonal evolution [136]. In such models, each cell has, for a given time unit, a probability to mutate and acquire metastatic ability, and then a probability to leave the primary tumor and establish a distant metastatic colony. Haeno et al. [136] applied their model to comprehensive data of pancreatic cancer patients and found that metastases were likely to be present at diagnosis. The model predictions also suggested that chemotherapy alone was better than surgery alone to maximize survival.

Perspectives for combining AI and mathematical modeling: mechanistic learning

While both dealing with relevant applications in clinical oncology, it is manifest that the works described within the two classes of mathematical modeling used above (AI and mechanistic modeling) have been performed by multiple communities (AI/ML, pharmacometrics, statistics, mathematicians) that have independently made progress but have remained partitioned. Bridging the gaps between disciplines would surely lead to more powerful methods able to improve the design of clinical trials and cancer patient care [142]. On one hand, the lack of interpretability of AI algorithms calls to "open the black box" and incorporate expert knowledge to design more biologically-informed models. On the other hand, most of mechanistic modeling studies have thus far dealt with variables in relatively low dimension but nevertheless face an increase in the amount of quantitative data produced. Therefore, they could benefit from AI techniques to integrate high-throughput data (e.g. omics or imaging data, beyond the mere size or volume of the lesions). For instance, instead of relying almost exclusively on linear covariate models (up to a transformation), highly nonlinear ML algorithms could be used to relate covariates and parameters of the structural model [143,144]. Another valuable approach is to derive quantitative metrics from simulation outputs of mechanistic modeling and use them as ML inputs for predictive purposes [145]. We propose to name such hybrid approaches combining big data and machine learning with mechanistic modeling "mechanistic learning" [85] (Figure 4).

An example of such mechanistic learning study was recently published for the prediction of metastatic relapse in early stage breast cancer [146]. Instead of using a biologically agnostic model for survival analysis (e.g. Cox or random survival forest), Nicolò et al. derived a mechanistic model for the actual time of relapse.

Moreover, in order to deal with the relatively large number of covariates (21), the authors relied on ML for feature selection. Comparison with classical or ML survival analysis revealed similar predictive power among the methods. However, the mechanistic approach presents the advantage to yield simulations of the patient's metastatic state.

Furthermore, the dimension of longitudinal data is increasing. While imaging data start to be analyzed longitudinally with techniques from AI (e.g., recurrent neural networks) [57], the advent of measurements from circulating tumor DNA provide an additional source of longitudinal high-dimensional data. So far, it remains an open question to design mechanistic models able to integrate such data. With the revolution of immunotherapy, increasing attention is given to molecular and cellular immune players. Data gathered from immune-monitoring (flow cytometry and seric markers) generate a large number (> 500) of quantitative variables measurable directly from blood samples, thus in a minimally-invasive manner that can be repeated. For instance, the PIONeeR project is a large-scale clinical study aiming at explaining primary or adaptive resistance to PD-1 inhibitors [147]. Such immune-monitoring data will be collected at multiple time points in patients during treatment. This data will further be modeled using a mechanistic learning approach in the QUANTIC project [147]. The objective is to build predictive tools able to leverage this high-dimensional data for personal predictions of the kinetics of response to treatment.

For efficient translation to the clinic, current mathematical modeling faces multiple challenges. First, it is highly dependent on data and requires large-scale curated databases. Molecular data are usually made publicly available upon publication of the results in online repositories such as the TCGA or GEO. Imaging data are also increasingly shared in similar repositories (see the TCIA [148] for radiological images or The Digital Slide Archive [149] for pathology images). However, individual-level data from clinical trials such as longitudinal lesion sizes, PK or biomarkers have limited availability, which is limiting the power of statistical and mechanistic modeling studies. Extending initiatives such as the

data sphere project [150] or Vivli (vivli.org), which proposes to share data from past clinical trials, would surely be very beneficial. Second, data sharing brings two issues: ethical and practical. The necessary ethical regulatory dispositions that have been introduced in the US (HIPAA) and Europe (GDPR) preserve patient privacy but also limit data sharing. Novel infrastructures enabling the development and testing of the models while ensuring security of the data have to be created [45]. Finally, while the wide arsenal of available anti-cancer therapies brings opportunities in terms of applications of mathematical modeling to optimize the design of combinatorial clinical trials, a current challenge is to develop mathematical models not only for clinical trials, but also for personalized therapy (Figure 3). To achieve this, structured and unstructured real-world data from routine management should be collected, organized, analyzed and made available to researchers, not only by private companies (e.g. Flatiron Health), but also public institutions [151]. Indeed, mathematical modeling is now well established for applications drug development, but further advances are needed to translate the use of the models at bedside.

Conclusion

Two hundred and sixty years after Bernoulli's model for vaccination, medicine, and particularly oncology, has never been closer to a quantitative science. Mathematical modeling, either purely statistical (AI), or mechanistic, has demonstrated that it is able to provide clinically relevant tools, whether for the improvement of clinical trials or personalized medicine. Hopefully, today's mathematical models will have a better future than Bernoulli's and an increasing number of these will be implemented into clinically actionable softwares for better patient care at bedside.

Application	Data	Method	Aim	Ref
Diagnosis	Single nucleotide polymorphisms (breast)	Support vector machines	Prediction of breast cancer	[22]
Diagnosis	Mammography (breast)	Deep learning	Breast cancer screening	[35]
Prognosis	Gene expression (breast)	Hierarchical clustering	Prediction of metastatic relapse	[15]
Prognosis	Pathology digital slides (colon)	Deep learning	Prediction of overall survival	[31]
Prediction of response	CT scans (multiple types)	Radiomics	Prediction of response to immunotherapy	[50]
Personalized medicine	Electronic health records	Natural language processing	Guide treatment decision at bedside	(-)

Table 1 : Case studies of artificial intelligence in clinical oncology

0

Application	Data	Method	Aim	Ref
Drug development	Preclinical	QSP	Determination of dose in FIH study	[80]
Drug development	Preclinical	QSP	Combination of radiotherapy and immune-checkpoint inhibition	[88]
Drug development/ Personalized medicine	Neutrophil counts	PK/PD	Design of clinical trial	[101]
Drug development	Tumor size and survival (lung)	TGI-OS	Prediction of phase III from phase II for Go/no-go decision	[122]
Prediction of response	Circulating biomarkers	PK/PD	Prediction of response to immunotherapy	[123]
Personalized medicine	Tumor size and survival (bladder)	Joint model	Individual prediction of survival	[124]
Prognosis	Clinico-pathologic biomarkers and metastasis-free survival (breast)	Metastasis model	Prediction of metastatic relapse	[146]

Table 2 : Case studies of mechanistic modeling in clinical oncology

FIH: first in human. PK: pharmacokinetics. PD: pharmacodynamics. TGI: tumor growth inhibition. OS: overall survival

Figure legends

Figure 1 : Artificial intelligence versus mechanistic modeling. Artificial intelligence algorithms act as poorly interpretable black boxes that process input 'big' data to generate predictive outputs, e.g for classification between high and low risk of survival or probability of response to therapy. In contrast, mechanistic models usually deal with lower-dimensional data (e.g., tumor size), but can provide simulations in addition to pure predictions. These include exploration of possible scenarii, for instance the impact of alternative scheduling regimen or the predicted amount of invisible metastases at time of diagnosis. TX = treatment.

Figure 2 : Overview of mechanistic methods in oncology. Departing from the dose (known), such models accommodate for four main types of quantitative data: drug concentrations, efficacy (e.g., tumor size), safety (e.g. neutrophil counts) and survival data. Mathematical tools developed to mine these data have varying degree of complexity, from elementary statistical analysis tools (e.g. logistic or Cox proportional hazard regression) in dose/exposure-response modeling, to advanced dynamic models based on differential equations in quantitative systems pharmacology.

POP PK: population pharmacokinetics. TGI: tumor growth inhibition.

Figure 3: Mechanistic modeling of brain metastasis in NSCLC [137]**. (**A) A mathematical model describing gompertzian primary tumor growth (two parameters), response to treatment through a tumor growth inhibition model (three parameters) and metastatic apparition and growth (two additional parameters) was able to describe longitudinal data on number and size of visible brain metastases from a patient with NSCLC. Time unit is months from

diagnosis. (B) Inferred size distributions of the total metastatic burden (visible + invisible) at time of primary tumor diagnosis. (C) Inferred size distributions of the total metastatic burden (visible + invisible) at time of first brain metastatic relapse.

PT = primary tumor. BM = brain metastasis. T_0 = time of first cancer cell. T_1 = time of diagnosis. T_2 = time of first brain metastatic relapse.

Figure 4 : Mechanistic learning. To account for the increasing dimension of the quantitative data able to feed mechanistic models, we propose to combine methods from machine learning (ML) and mechanistic modeling. The link between high-dimensional baseline data (demographic, clinical, pathological, molecular or biological variables) and model parameters could be achieved with ML algorithms. Longitudinal data (e.g. tumor size measurements, pharmacokinetics, immune-monitoring, seric biomarkers or circulating DNA), possibly in large dimension as well, are incorporated using mixed-effects modeling. Time-to-event data (e.g., progression-free or overall survival) could also be modeled with a mechanistic basis (instead of biologically-agnostic survival analysis based on, e.g., Cox regression). Once calibrated, the mechanistic model can be used to simulate the impact of candidate scheduling regimen to guide clinical trials, or help treatment individualization.

References

1. Bray, F. *et al.* Global cancer statistics 2018: GLOBOCAN estimates of incidence and mortality worldwide for 36 cancers in 185 countries. *CA: A Cancer Journal for Clinicians* **68**, 394–424 (2018).

2. Wigner, E. P. The unreasonable effectiveness of mathematics in the natural sciences. Richard courant lecture in mathematical sciences delivered at New York University, May 11, 1959. *Communications on Pure and Applied Mathematics* **13**, 1–14 (1960).

3. Bernoulli, D. Essai d'une nouvelle analyse de la mortalité causée par la petite vérole, et des avantages de l'inoculation pour la prévenir. *Histoire de l'Acad., Roy. Sci.(Paris) avec Mem* 1–45 (1760).

4. Gatenby, R. A. & Maini, P. K. Mathematical oncology: cancer summed up. *Nature* **421**, 321–321 (2003).

5. Barbolosi, D., Ciccolini, J., Lacarelle, B., Barlési, F. & André, N. Computational oncology—mathematical modelling of drug regimens for precision medicine. *Nature reviews Clinical oncology* **13**, 242 (2016).

6. Altrock, P. M., Liu, L. L. & Michor, F. The mathematics of cancer: integrating quantitative models. *Nat Rev Cancer* **15**, 730–745 (2015).

7. Kourou, K., Exarchos, T. P., Exarchos, K. P., Karamouzis, M. V. & Fotiadis, D. I. Machine learning applications in cancer prognosis and prediction. *Comput Struct Biotechnol J* **13**, 8–17 (2015).

8. Simon, N., Friedman, J., Hastie, T. & Tibshirani, R. Regularization Paths for Cox's Proportional Hazards Model via Coordinate Descent. *J. Stat. Soft.* **39**, (2011).

9. LeCun, Y., Bengio, Y. & Hinton, G. Deep learning. *Nature* **521**, 436–444 (2015).

10. Topol, E. J. High-performance medicine: the convergence of human and artificial intelligence. *Nat Med* **25**, 44 (2019).

11. Barrett, T. *et al.* NCBI GEO: archive for functional genomics data sets—update. *Nucleic Acids Res* **41**, D991–D995 (2013).

12. Golub, T. R. *et al.* Molecular classification of cancer: class discovery and class prediction by gene expression monitoring. *Science* **286**, 531–537 (1999).

13. Ramaswamy, S. *et al.* Multiclass cancer diagnosis using tumor gene expression signatures. *Proc Natl Acad Sci USA* **98**, 15149–15154 (2001).

14. Perou, C. M. *et al.* Molecular portraits of human breast tumours. *Nature* **406**, 747–752 (2000).

15. Veer, L. J. van 't *et al.* Gene expression profiling predicts clinical outcome of breast cancer. *Nature* **415**, 530–536 (2002).

16. Shedden, K. *et al.* Gene expression–based survival prediction in lung adenocarcinoma: a multi-site, blinded validation study. *Nat Med* **14**, 822–827 (2008).

17. Guinney, J. *et al.* The consensus molecular subtypes of colorectal cancer. *Nat. Med.* **21**, 1350–1356 (2015).

18. Capper, D. *et al.* DNA methylation-based classification of central nervous system tumours. *Nature* **555**, 469–474 (2018).

19. Eisen, M. B., Spellman, P. T., Brown, P. O. & Botstein, D. Cluster analysis and display of genome-wide expression patterns. *Proc Natl Acad Sci USA* **95**, 14863–14868 (1998).

20. Alexe, G., Dalgin, G. S., Ganesan, S., Delisi, C. & Bhanot, G. Analysis of breast cancer progression using principal component analysis and clustering. *J. Biosci.* **32**, 1027–1039 (2007).

21. IJzendoorn, D. G. P. van *et al.* Machine learning analysis of gene expression data reveals novel diagnostic and prognostic biomarkers and identifies therapeutic targets for soft tissue sarcomas. *PLoS Comput Biol* **15**, e1006826 (2019).

22. Listgarten, J. *et al.* Predictive Models for Breast Cancer Susceptibility from Multiple Single Nucleotide Polymorphisms. *Clin Cancer Res* **10**, 2725–2737 (2004).

23. Zhu, W., Xie, L., Han, J. & Guo, X. The Application of Deep Learning in Cancer Prognosis Prediction. *Cancers* **12**, 603 (2020).

24. Ching, T., Zhu, X. & Garmire, L. X. Cox-nnet: An artificial neural network method for prognosis prediction of high-throughput omics data. *PLoS Comput Biol* **14**, e1006076 (2018).

25. Chaudhary, K., Poirion, O. B., Lu, L. & Garmire, L. X. Deep Learning-Based Multi-Omics Integration Robustly Predicts Survival in Liver Cancer. *Clin. Cancer Res.* **24**, 1248–1259 (2018).

26. Huang, Z. *et al.* SALMON: Survival Analysis Learning With Multi-Omics Neural Networks on Breast Cancer. *Front Genet* **10**, 166 (2019).

27. Yousefi, S. *et al.* Predicting clinical outcomes from large scale cancer genomic profiles with deep survival models. *Sci Rep* **7**, 1–11 (2017).

28. Esteva, A. *et al.* Dermatologist-level classification of skin cancer with deep neural networks. *Nature* **542**, 115–118 (2017).

29. Liu, Y. *et al.* Artificial Intelligence-Based Breast Cancer Nodal Metastasis Detection: Insights Into the Black Box for Pathologists. *Arch. Pathol. Lab. Med.* **143**, 859–868 (2019).

30. Chen, P.-H. C. *et al.* An augmented reality microscope with real-time artificial intelligence integration for cancer diagnosis. *Nature Medicine* **25**, 1453–1457 (2019).

31. Kather, J. N. *et al.* Predicting survival from colorectal cancer histology slides using deep learning: A retrospective multicenter study. *PLOS Medicine* **16**, e1002730 (2019).

32. Kather, J. N. *et al.* Deep learning can predict microsatellite instability directly from histology in gastrointestinal cancer. *Nat. Med.* **25**, 1054–1056 (2019).

33. Coudray, N. *et al.* Classification and mutation prediction from non-small cell lung cancer histopathology images using deep learning. *Nat. Med.* **24**, 1559–1567 (2018).

34. Courtiol, P. *et al.* Deep learning-based classification of mesothelioma improves prediction of patient outcome. *Nature Medicine* **25**, 1519–1525 (2019).

35. McKinney, S. M. *et al.* International evaluation of an AI system for breast cancer screening. *Nature* **577**, 89–94 (2020).

36. Wu, N. *et al.* Deep Neural Networks Improve Radiologists' Performance in Breast Cancer Screening. *IEEE Trans Med Imaging* 1–1 (2019).doi:10.1109/TMI.2019.2945514

37. Ardila, D. *et al.* End-to-end lung cancer screening with three-dimensional deep learning on low-dose chest computed tomography. *Nature Medicine* **25**, 954–961 (2019).

38. Shin, H.-C. *et al.* Deep Convolutional Neural Networks for Computer-Aided Detection: CNN Architectures, Dataset Characteristics and Transfer Learning. *IEEE Trans Med Imaging* **35**, 1285–1298 (2016).

39. Setio, A. A. A. *et al.* Validation, comparison, and combination of algorithms for automatic detection of pulmonary nodules in computed tomography images: The LUNA16 challenge. *Medical Image Analysis* **42**, 1–13 (2017).

40. Vorontsov, E. *et al.* Deep Learning for Automated Segmentation of Liver Lesions at CT in Patients with Colorectal Cancer Liver Metastases. *Radiology: Artificial Intelligence* **1**, 180014 (2019).

41. Pereira, S., Pinto, A., Alves, V. & Silva, C. A. Brain Tumor Segmentation Using Convolutional Neural Networks in MRI Images. *IEEE Transactions on Medical Imaging* **35**, 1240–1251 (2016).

42. Griethuysen, J. J. M. van *et al.* Computational Radiomics System to Decode the Radiographic Phenotype. *Cancer Res* **77**, e104–e107 (2017).

43. Nioche, C. *et al.* LIFEx: a freeware for radiomic feature calculation in multimodality imaging to accelerate advances in the characterization of tumor heterogeneity. *Cancer Res* **78**, canres.0125.2018-4789 (2018).

44. Lambin, P. *et al.* Radiomics: extracting more information from medical images using advanced feature analysis. *Eur J Cancer* **48**, 441–446 (2012).

45. Hosny, A., Parmar, C., Quackenbush, J., Schwartz, L. H. & Aerts, H. J. W. L. Artificial intelligence in radiology. *Nature Reviews Cancer* **18**, 500–510 (2018).

46. Coroller, T. P. *et al.* CT-based radiomic signature predicts distant metastasis in lung adenocarcinoma. *Radiotherapy and Oncology* **114**, 345–350 (2015).

47. Velazquez, E. R. *et al.* Somatic Mutations Drive Distinct Imaging Phenotypes in Lung Cancer. *Cancer Res* **77**, 3922–3930 (2017).

48. Grossmann, P. *et al.* Defining the biological basis of radiomic phenotypes in lung cancer. *Elife* **6**, (2017).

49. Crombé, A. *et al.* T2 -based MRI Delta-radiomics improve response prediction in soft-tissue sarcomas treated by neoadjuvant chemotherapy. *J Magn Reson Imaging* **50**, 497–510 (2019).

50. Sun, R. *et al.* A radiomics approach to assess tumour-infiltrating CD8 cells and response to anti-PD-1 or anti-PD-L1 immunotherapy: an imaging biomarker, retrospective multicohort study. *Lancet Oncol* **19**, 1180–1191 (2018).

51. Welch, M. L. *et al.* Vulnerabilities of radiomic signature development: The need for safeguards. *Radiother Oncol* **130**, 2–9 (2019).

52. Peng, H. *et al.* Prognostic Value of Deep Learning PET/CT-based Radiomics: Potential Role for Future Individual Induction Chemotherapy in Advanced Nasopharyngeal Carcinoma. *Clin Cancer Res* (2019).doi:10.1158/1078-0432.CCR-18-3065

53. Hosny, A. *et al.* Deep learning for lung cancer prognostication: A retrospective multi-cohort radiomics study. *PLoS Med* **15**, (2018).

54. Lao, J. *et al.* A Deep Learning-Based Radiomics Model for Prediction of Survival in Glioblastoma Multiforme. *Sci Rep* **7**, 10353 (2017).

55. Wang, H. *et al.* Comparison of machine learning methods for classifying

mediastinal lymph node metastasis of non-small cell lung cancer from 18F-FDG PET/CT images. *EJNMMI Research* **7**, 11 (2017).

56. Cha, K. H. *et al.* Bladder Cancer Treatment Response Assessment in CT using Radiomics with Deep-Learning. *Sci Rep* **7**, 8738 (2017).

57. Xu, Y. *et al.* Deep Learning Predicts Lung Cancer Treatment Response from Serial Medical Imaging. *Clin Cancer Res* **25**, 3266–3275 (2019).

58. Somashekhar, S. P. *et al.* Watson for Oncology and breast cancer treatment recommendations: agreement with an expert multidisciplinary tumor board. *Ann Oncol* **29**, 418–423 (2018).

59. Lee, W.-S. *et al.* Assessing Concordance With Watson for Oncology, a Cognitive Computing Decision Support System for Colon Cancer Treatment in Korea. *JCO Clin Cancer Inform* **2**, 1–8 (2018).

60. IBM pitched Watson as a revolution in cancer care. It's nowhere close. *STAT* (2017).at <https://www.statnews.com/2017/09/05/watson-ibm-cancer/>

61. Yu, M. K. *et al.* Visible Machine Learning for Biomedicine. *Cell* **173**, 1562–1565 (2018).

62. Tang, J., Shalabi, A. & Hubbard-Lucey, V. M. Comprehensive analysis of the clinical immuno-oncology landscape. *Ann Oncol* **29**, 84–91 (2018).

63. Sheiner, L. B., Rosenberg, B. & Melmon, K. L. Modelling of individual pharmacokinetics for computer-aided drug dosage. *Computers and Biomedical Research* **5**, 441–459 (1972).

64. Bajaj, G. *et al.* Model-Based Population Pharmacokinetic Analysis of Nivolumab in Patients With Solid Tumors. *CPT Pharmacometrics Syst Pharmacol* **6**, 58–66 (2017).

65. Liu, C. *et al.* Association of time-varying clearance of nivolumab with disease dynamics and its implications on exposure response analysis. *Clin. Pharmacol. Ther.* **101**, 657–666 (2017).

66. Li, H. *et al.* Time dependent pharmacokinetics of pembrolizumab in patients with solid tumor and its correlation with best overall response. *J Pharmacokinet Pharmacodyn* **44**, 403–414 (2017).

67. Feng, Y. *et al.* Model-based clinical pharmacology profiling of ipilimumab in patients with advanced melanoma. *Br J Clin Pharmacol* **78**, 106–117 (2014).

68. Sanghavi, K. *et al.* Population Pharmacokinetics of Ipilimumab in Combination With Nivolumab in Patients With Advanced Solid Tumors. *CPT: Pharmacometrics & Systems Pharmacology* **9**, 29–39 (2020).

69. Ahamadi, M. *et al.* Model-Based Characterization of the Pharmacokinetics of Pembrolizumab: A Humanized Anti-PD-1 Monoclonal Antibody in Advanced Solid Tumors. *CPT Pharmacometrics Syst Pharmacol* **6**, 49–57 (2017).

70. Stroh, M. *et al.* Clinical Pharmacokinetics and Pharmacodynamics of Atezolizumab in Metastatic Urothelial Carcinoma. *Clin. Pharmacol. Ther.* **102**, 305–312 (2017).

71. Baverel, P. G. *et al.* Population Pharmacokinetics of Durvalumab in Cancer Patients and Association With Longitudinal Biomarkers of Disease Status. *Clin. Pharmacol. Ther.* **103**, 631–642 (2018).

72. Ratain, M. J. & Goldstein, D. A. Time Is Money: Optimizing the Scheduling of Nivolumab. *J Clin Oncol* JCO.18.00045-4 (2018).doi:10.1200/JCO.18.00045

73. Feng, Y. *et al.* Exposure–response relationships of the efficacy and safety of ipilimumab in patients with advanced melanoma. *Clin Cancer Res* **19**, 3977–3986 (2013).

74. Wang, X. *et al.* Quantitative Characterization of the Exposure-Response Relationship for Cancer Immunotherapy: A Case Study of Nivolumab in Patients With Advanced Melanoma. *CPT Pharmacometrics Syst Pharmacol* **6**, 40–48 (2017).

75. Feng, Y. *et al.* Nivolumab Exposure–Response Analyses of Efficacy and Safety in Previously Treated Squamous or Nonsquamous Non–Small Cell Lung Cancer. *Clin Cancer Res* **23**, 5394–5405 (2017).

76. Turner, D. C. *et al.* Pembrolizumab Exposure–Response Assessments Challenged by Association of Cancer Cachexia and Catabolic Clearance. *Clin Cancer Res* (2018).doi:10.1158/1078-0432.CCR-18-0415

77. Morrissey, K. M. *et al.* Alternative dosing regimens for atezolizumab: an example of model-informed drug development in the postmarketing setting. *Cancer Chemother Pharmacol* **84**, 1257–1267 (2019).

78. Long, G. V. *et al.* Assessment of nivolumab exposure and clinical safety of 480 mg every 4 weeks flat-dosing schedule in patients with cancer. *Ann Oncol* **29**, 2208–2213 (2018).

79. Zhao, X., Wang, X., Feng, Y., Agrawal, S. & Shah, D. K. Application of PK-PD Modeling and Simulation Approaches for Immuno-Oncology Drugs. In *Development of Antibody-Based Therapeutics* **4**, 207–222 (Adis, Singapore, Singapore, 2018).

80. Lindauer, A. *et al.* Translational pharmacokinetic/pharmacodynamic modeling of tumor growth inhibition supports dose-range selection of the anti–PD-1 antibody pembrolizumab. *CPT Pharmacometrics Syst Pharmacol* **6**, 11–20 (2017).

81. Chatterjee, M. S. *et al.* Population Pharmacokinetic/Pharmacodynamic Modeling of Tumor Size Dynamics in Pembrolizumab-Treated Advanced Melanoma. *CPT Pharmacometrics Syst Pharmacol* **6**, 29–39 (2017).

82. Ribba, B. *et al.* Prediction of the Optimal Dosing Regimen Using a Mathematical Model of Tumor Uptake for Immunocytokine-Based Cancer Immunotherapy. *Clin Cancer Res* **24**, 3325–3333 (2018).

83. Sharma, P., Hu-Lieskovan, S., Wargo, J. A. & Ribas, A. Primary, Adaptive, and Acquired Resistance to Cancer Immunotherapy. *Cell* **168**, 707–723 (2017).

84. Palmer, A. C. & Sorger, P. K. Combination Cancer Therapy Can Confer Benefit via Patient-to-Patient Variability without Drug Additivity or Synergy. *Cell* **171**, 1678-1691.e13 (2017).

85. Ciccolini, J., Barbolosi, D., André, N., Barlesi, F. & Benzekry, S. Mechanistic Learning for Combinatorial Strategies With Immuno-oncology Drugs: Can Model-

Informed Designs Help Investigators? *JCO Precision Oncology* 486–491 (2020).doi:10.1200/PO.19.00381

86. Milberg, O. *et al.* A QSP Model for Predicting Clinical Responses to Monotherapy, Combination and Sequential Therapy Following CTLA-4, PD-1, and PD-L1 Checkpoint Blockade. *Scientific Reports* **9**, 11286 (2019).

87. Serre, R. *et al.* Mathematical Modeling of Cancer Immunotherapy and Its Synergy with Radiotherapy. *Cancer Res* **76**, 4931–4940 (2016).

88. Kosinsky, Y. *et al.* Radiation and PD-(L)1 treatment combinations: immune response and dose optimization via a predictive systems model. *J Immunother Cancer* **6**, 17 (2018).

89. Serre, R., Barlesi, F., Muracciole, X. & Barbolosi, D. Immunologically effective dose: a practical model for immuno-radiotherapy. *Oncotarget* **9**, 31812–31819 (2018).

90. Antonia, S. J. *et al.* Durvalumab after Chemoradiotherapy in Stage III Non–Small-Cell Lung Cancer. *N Engl J Med* **377**, 1919–1929 (2017).

91. Wilson, S. *et al.* Modeling and predicting optimal treatment scheduling between the antiangiogenic drug sunitinib and irinotecan in preclinical settings. *CPT Pharmacometrics Syst. Pharmacol.* **4**, 720–727 (2015).

92. Imbs, D.-C. *et al.* Revisiting Bevacizumab + Cytotoxics Scheduling Using Mathematical Modeling: Proof of Concept Study in Experimental Non-Small Cell Lung Carcinoma. *CPT Pharmacometrics Syst Pharmacol* **7**, 42–50 (2018).

93. Benzekry, S. *et al.* Metronomic reloaded: Theoretical models bringing chemotherapy into the era of precision medicine. *Semin Cancer Biol* **35**, 53–61 (2015).

94. Skipper, H. E., Schabel, F. M. & Wilcox, W. S. Experimental evaluation of potential anticancer agents XIII. On the criteria and kinetics associated with 'curability' of experimental leukemia. *Cancer Chemother Rep* **35**, 1–111 (1964).

95. Jusko, W. J. Pharmacodynamics of Chemotherapeutic Effects: Dose-Time-Response Relationships for Phase-Nonspecific Agents. *JPharmSci* **60**, 892–895 (1971).

96. Jusko, W. J. A pharmacodynamic model for cell-cycle-specific chemotherapeutic agents. *Journal of Pharmacokinetics and Biopharmaceutics* **1**, 175–200 (1973).

97. Norton, L. & Simon, R. Tumor size, sensitivity to therapy, and design of treatment schedules. *Cancer Treat Rep* **61**, 1307–1317 (1977).

98. Norton, L. A Gompertzian model of human breast cancer growth. *Cancer Res* **48**, 7067–7071 (1988).

99. Citron, M. L. *et al.* Randomized trial of dose-dense versus conventionally scheduled and sequential versus concurrent combination chemotherapy as postoperative adjuvant treatment of node-positive primary breast cancer: first report of Intergroup Trial C9741/Cancer and Leukemia Group B Trial 9741. *J Clin Oncol* **21**, 1431–1439 (2003).

100. Friberg, L. E., Henningsson, A., Maas, H., Nguyen, L. & Karlsson, M. O. Model of chemotherapy-induced myelosuppression with parameter consistency across drugs. *J. Clin. Oncol.* **20**, 4713–4721 (2002).

101. Meille, C., Barbolosi, D., Ciccolini, J., Freyer, G. & Iliadis, A. Revisiting Dosing Regimen Using Pharmacokinetic/Pharmacodynamic Mathematical Modeling: Densification and Intensification of Combination Cancer Therapy. *Clin Pharmacokinet* **55**, 1015–1025 (2016).

102. Hénin, E. *et al.* Revisiting dosing regimen using PK/PD modeling: the MODEL1 phase I/II trial of docetaxel plus epirubicin in metastatic breast cancer patients. *Breast Cancer Res Treat* **156**, 331–341 (2016).

103. Barlesi, F. *et al.* Mathematical modeling for Phase I cancer trials: A study of metronomic vinorelbine for advanced non-small cell lung cancer (NSCLC) and mesothelioma patients. *Oncotarget* **8**, 47161–47166 (2017).

104. Gerlinger, M. *et al.* Intratumor heterogeneity and branched evolution revealed by multiregion sequencing. *N. Engl. J. Med.* **366**, 883–892 (2012).

105. Goldie, J. H. & Coldman, a J. A mathematic model for relating the drug

sensitivity of tumors to their spontaneous mutation rate. *Cancer Treat Rep* **63**, 1727–1733 (1979).

106. Chmielecki, J. *et al.* Optimization of dosing for EGFR-mutant non-small cell lung cancer with evolutionary cancer modeling. *Sci Transl Med* **3**, 90ra59-90ra59 (2011).

107. Yu, H. A. *et al.* Phase 1 study of twice weekly pulse dose and daily low-dose erlotinib as initial treatment for patients with EGFR-mutant lung cancers. *Ann Oncol* **28**, 278–284 (2017).

108. Gatenby, R. A. A change of strategy in the war on cancer. *Nature* **459**, 508–509 (2009).

109. Foo, J. & Michor, F. Evolution of resistance to targeted anti-cancer therapies during continuous and pulsed administration strategies. *PLoS Comput Biol* **5**, e1000557 (2009).

110. Gatenby, R. a, Silva, A. S., Gillies, R. J. & Frieden, B. R. Adaptive therapy. *Cancer Res* **69**, 4894–4903 (2009).

111. Enriquez-Navas, P. M. *et al.* Exploiting evolutionary principles to prolong tumor control in preclinical models of breast cancer. *Sci Transl Med* **8**, 327ra24 (2016).

112. Zhang, J., Cunningham, J. J., Brown, J. S. & Gatenby, R. a Integrating evolutionary dynamics into treatment of metastatic castrate-resistant prostate cancer. *Nature Communications* **8**, 1816 (2017).

113. Eisenhauer, E. A. *et al.* New response evaluation criteria in solid tumours: Revised RECIST guideline (version 1.1). *European Journal of Cancer* **45**, 228–247 (2009).

114. Feng, Y., Wang, X., Suryawanshi, S., Bello, A. & Roy, A. Linking Tumor Growth Dynamics to Survival in Ipilimumab-Treated Patients With Advanced Melanoma Using Mixture Tumor Growth Dynamic Modeling. *CPT Pharmacometrics Syst Pharmacol* **8**, 825–834 (2019).

115. Tham, L.-S. *et al.* A Pharmacodynamic Model for the Time Course of Tumor Shrinkage by Gemcitabine + Carboplatin in Non–Small Cell Lung Cancer Patients. *Clin Cancer Res* **14**, 4213–4218 (2008).

116. Wang, Y. *et al.* Elucidation of relationship between tumor size and survival in non-small-cell lung cancer patients can aid early decision making in clinical drug development. *Clin Pharmacol Ther* **86**, 167–174 (2009).

117. Claret, L. *et al.* Model-based prediction of phase III overall survival in colorectal cancer on the basis of phase II tumor dynamics. *J Clin Oncol* **27**, 4103–4108 (2009).

118. Stein, W. D. *et al.* Tumor growth rates derived from data for patients in a clinical trial correlate strongly with patient survival: a novel strategy for evaluation of clinical trial data. *The Oncologist* **13**, 1046–1054 (2008).

119. Bruno, R. *et al.* Progress and Opportunities to Advance Clinical Cancer Therapeutics Using Tumor Dynamic Models. *Clin Cancer Res* 1–22 (2019).doi:10.1158/1078-0432.CCR-19-0287

120. Ribba, B. *et al.* A tumor growth inhibition model for low-grade glioma treated with chemotherapy or radiotherapy. *Clin Cancer Res* **18**, 5071–80 (2012).

121. Zheng, Y. *et al.* Population Modeling of Tumor Kinetics and Overall Survival to Identify Prognostic and Predictive Biomarkers of Efficacy for Durvalumab in Patients With Urothelial Carcinoma. *Clin Pharmacol Ther* **103**, 643–652 (2018).

122. Claret, L. *et al.* A Model of Overall Survival Predicts Treatment Outcomes with Atezolizumab versus Chemotherapy in Non-Small Cell Lung Cancer Based on Early Tumor Kinetics. *Clin Cancer Res* **24**, 3292–3298 (2018).

123. Netterberg, I. *et al.* A PK/PDAnalysis of Circulating Biomarkers and Their Relationship to Tumor Response in Atezolizumab-Treated non-small Cell Lung Cancer Patients. *Clin Pharmacol Ther* **105**, 486–495 (2018).

124. Tardivon, C. *et al.* Association Between Tumor Size Kinetics and Survival in Patients With Urothelial Carcinoma Treated With Atezolizumab: Implication for Patient Follow-Up. *Clin Pharmacol Ther* **106**, 810–820 (2019).

125. Netterberg, I. *et al.* Tumor Time-Course Predicts Overall Survival in Non-Small Cell Lung Cancer Patients Treated with Atezolizumab: Dependency on Follow-Up Time. *CPT Pharmacometrics Syst Pharmacol* psp4.12489 (2020).doi:10.1002/psp4.12489

126. Desmée, S., Mentré, F., Veyrat-Follet, C. & Guedj, J. Nonlinear Mixed-Effect Models for Prostate-Specific Antigen Kinetics and Link with Survival in the Context of Metastatic Prostate Cancer: a Comparison by Simulation of Two-Stage and Joint Approaches. *AAPS J* **17**, 691–699 (2015).

127. Król, A., Tournigand, C., Michiels, S. & Rondeau, V. Multivariate joint frailty model for the analysis of nonlinear tumor kinetics and dynamic predictions of death. *Stat Med* **37**, 2148–2161 (2018).

128. Proust-Lima, C. & Taylor, J. M. G. Development and validation of a dynamic prognostic tool for prostate cancer recurrence using repeated measures of posttreatment PSA: a joint modeling approach. *Biostatistics* **10**, 535–549 (2009).

129. Benzekry, S., Lamont, C., Barbolosi, D., Hlatky, L. & Hahnfeldt, P. Mathematical Modeling of Tumor-Tumor Distant Interactions Supports a Systemic Control of Tumor Growth. *Cancer Res* **77**, 5183–5193 (2017).

130. Claret, L. *et al.* Comparison of tumor size assessments in tumor growth inhibition-overall survival models with second-line colorectal cancer data from the VELOUR study. *Cancer Chemother Pharmacol* **82**, 49–54 (2018).

131. Mistry, H. B., Helmlinger, G., Al-Huniti, N., Vishwanathan, K. & Yates, J. Resistance models to EGFR inhibition and chemotherapy in non-small cell lung cancer via analysis of tumour size dynamics. *Cancer Chemother Pharmacol* (2019).doi:10.1007/s00280-019-03840-3

132. Hartung, N. *et al.* Study of metastatic kinetics in metastatic melanoma treated with B-RAF inhibitors: Introducing mathematical modelling of kinetics into the therapeutic decision. *PLoS ONE* **12**, e0176080 (2017).

133. Schindler, E. *et al.* Pharmacometric Modeling of Liver Metastases' Diameter,

Volume, and Density and Their Relation to Clinical Outcome in Imatinib-Treated Patients With Gastrointestinal Stromal Tumors. *CPT: Pharmacometrics & Systems Pharmacology* **6**, 449–457 (2017).

134. Schindler, E., Amantea, M. A., Karlsson, M. O. & Friberg, L. E. PK-PD modeling of individual lesion FDG-PET response to predict overall survival in patients with sunitinib-treated gastrointestinal stromal tumor. *CPT: Pharmacometrics & Systems Pharmacology* **5**, 173–181 (2016).

135. Iwata, K., Kawasaki, K. & Shigesada, N. A Dynamical Model for the Growth and Size Distribution of Multiple Metastatic Tumors. *J Theor Biol* **203**, 177–186 (2000).

136. Haeno, H. *et al.* Computational Modeling of Pancreatic Cancer Reveals Kinetics of Metastasis Suggesting Optimum Treatment Strategies. *Cell* **148**, 362–375 (2012).

137. Bilous, M. *et al.* Quantitative mathematical modeling of clinical brain metastasis dynamics in non-small cell lung cancer. *Sci Rep* **9**, 13018 (2019).

138. Hartung, N. *et al.* Mathematical modeling of tumor growth and metastatic spreading: validation in tumor-bearing mice. *Cancer Res* **74**, 6397–6407 (2014).

139. Benzekry, S. *et al.* Modeling Spontaneous Metastasis following Surgery: An In Vivo-In Silico Approach. *Cancer Res* **76**, 535–547 (2016).

140. Retsky, M. W. *et al.* Computer simulation of a breast cancer metastasis model. *Breast Cancer Res Treat* **45**, 193–202 (1997).

141. Hanin, L., Seidel, K. & Stoevesandt, D. A "universal" model of metastatic cancer, its parametric forms and their identification: what can be learned from site-specific volumes of metastases. *J Math Biol* **72**, 1633–1662 (2016).

142. Mentré, F. *et al.* Pharmacometrics and Systems Pharmacology 2030. *Clinical Pharmacology & Therapeutics* **107**, 76–78 (2020).

143. Lai, T. L., Shih, M.-C. & Wong, S. P. A new approach to modeling covariate effects and individualization in population pharmacokinetics-pharmacodynamics. *J Pharmacokinet Pharmacodyn* **33**, 49–74 (2006).

144. Knights, J. *et al.* Vertical Integration of Pharmacogenetics in Population PK/PD Modeling: A Novel Information Theoretic Method. *CPT: Pharmacometrics & Systems Pharmacology* **2**, 25 (2013).

145. Lancaster, M. C. & Sobie, E. A. Improved Prediction of Drug-Induced Torsades de Pointes Through Simulations of Dynamics and Machine Learning Algorithms. *Clin. Pharmacol. Ther.* **100**, 371–379 (2016).

146. Nicolò, C. *et al.* Machine Learning and Mechanistic Modeling for Prediction of Metastatic Relapse in Early-Stage Breast Cancer. *JCO Clin Cancer Inform* **4**, 259–274 (2020).

147. Ciccolini, J., Benzekry, S. & Barlesi, F. Deciphering response and resistance to immunecheckpoint inhibitors in lung cancer with artificial intelligence-based analysis: the PIONeeR and QUANTIC projects. *British Journal of Cancer* **under review**, (2020).

148. Clark, K. *et al.* The Cancer Imaging Archive (TCIA): Maintaining and Operating a Public Information Repository. *J Digit Imaging* **26**, 1045–1057 (2013).

149. Gutman, D. A. *et al.* The Digital Slide Archive: A Software Platform for Management, Integration, and Analysis of Histology for Cancer Research. *Cancer Res.* **77**, e75–e78 (2017).

150. Hede, K. Project Data Sphere to Make Cancer Clinical Trial Data Publicly Available. *J Natl Cancer Inst* **105**, 1159–1160 (2013).

151. NCI Cancer Research Data Commons | CBIIT. at <https://datascience.cancer.gov/data-commons>

CLINICAL DATA

IMAGING DATA

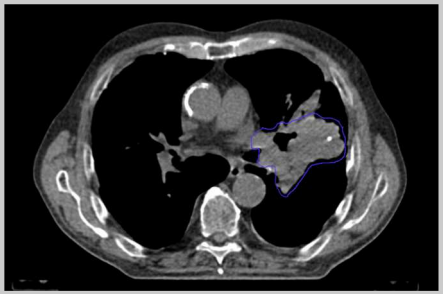

MOLECULAR DATA (OMICS)

ARTIFICIAL INTELLIGENCE

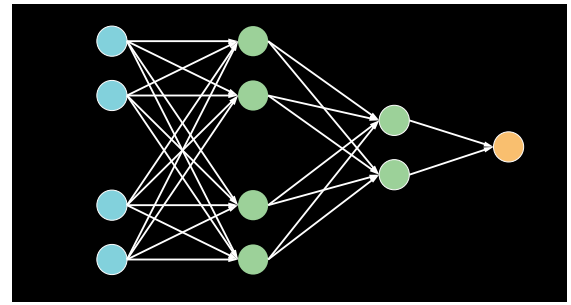

PREDICTION

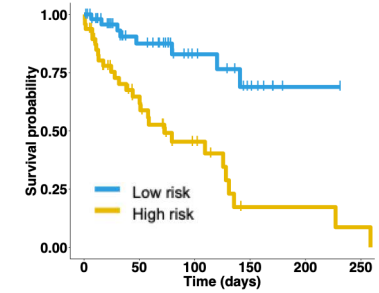

MECHANISTIC MODEL

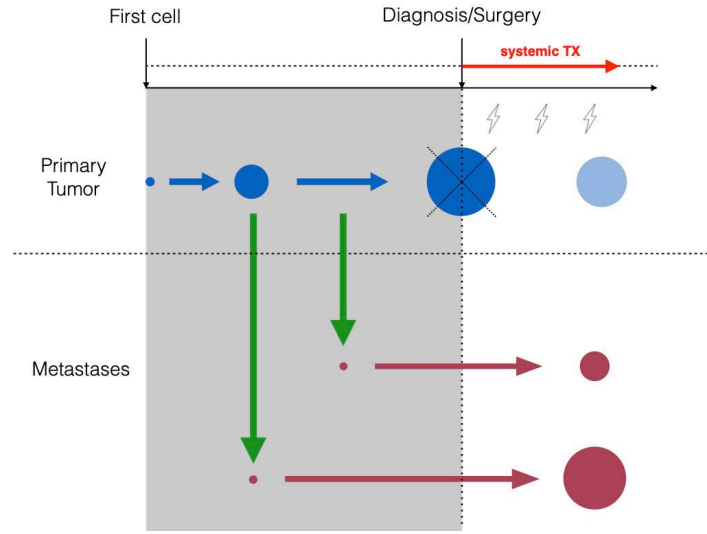

PREDICTION

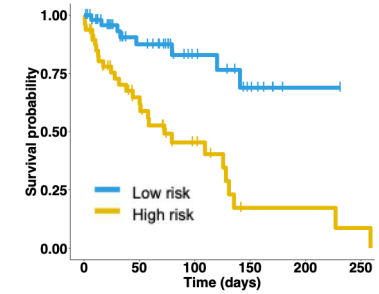

SIMULATION

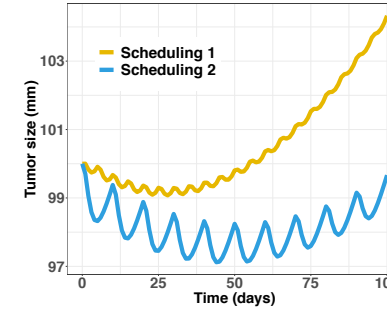

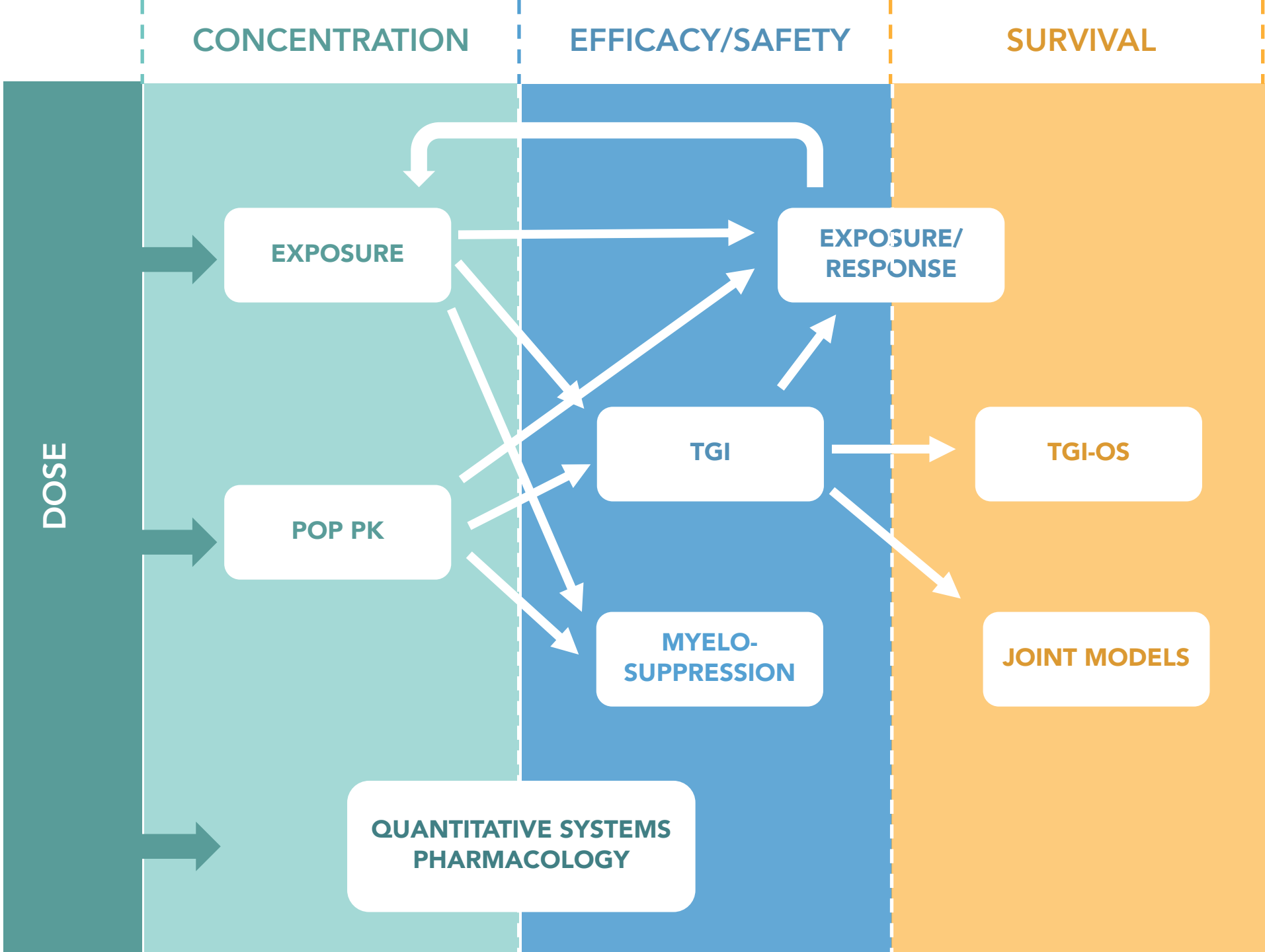
CONCENTRATION
EFFICACY/SAFETY
SURVIVAL
DOSE
EXPOSURE
EXPOSURE/
RESPONSE
TGI
TGI-OS
POP PK
MYELO-
SUPPRESSION
JOINT MODELS
QUANTITATIVE SYSTEMS
PHARMACOLOGY

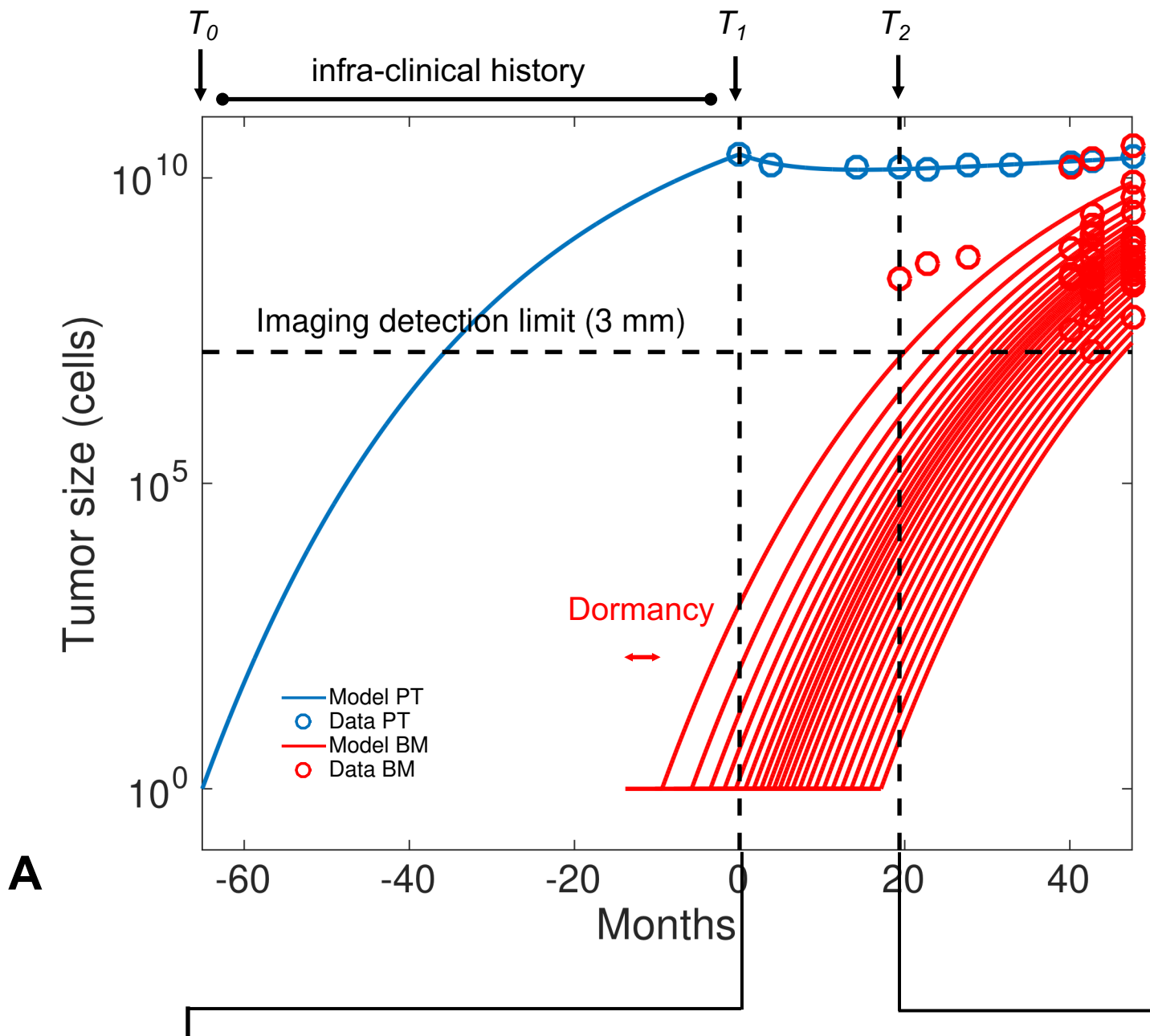
T_0
T_1
T_2
infra-clinical history
10^{10}
10^5
10^0
Tumor size (cells)
Imaging detection limit (3 mm)
Dormancy
Model PT
Data PT
Model BM
Data BM
-60
-40
-20
0
20
40
Months

A

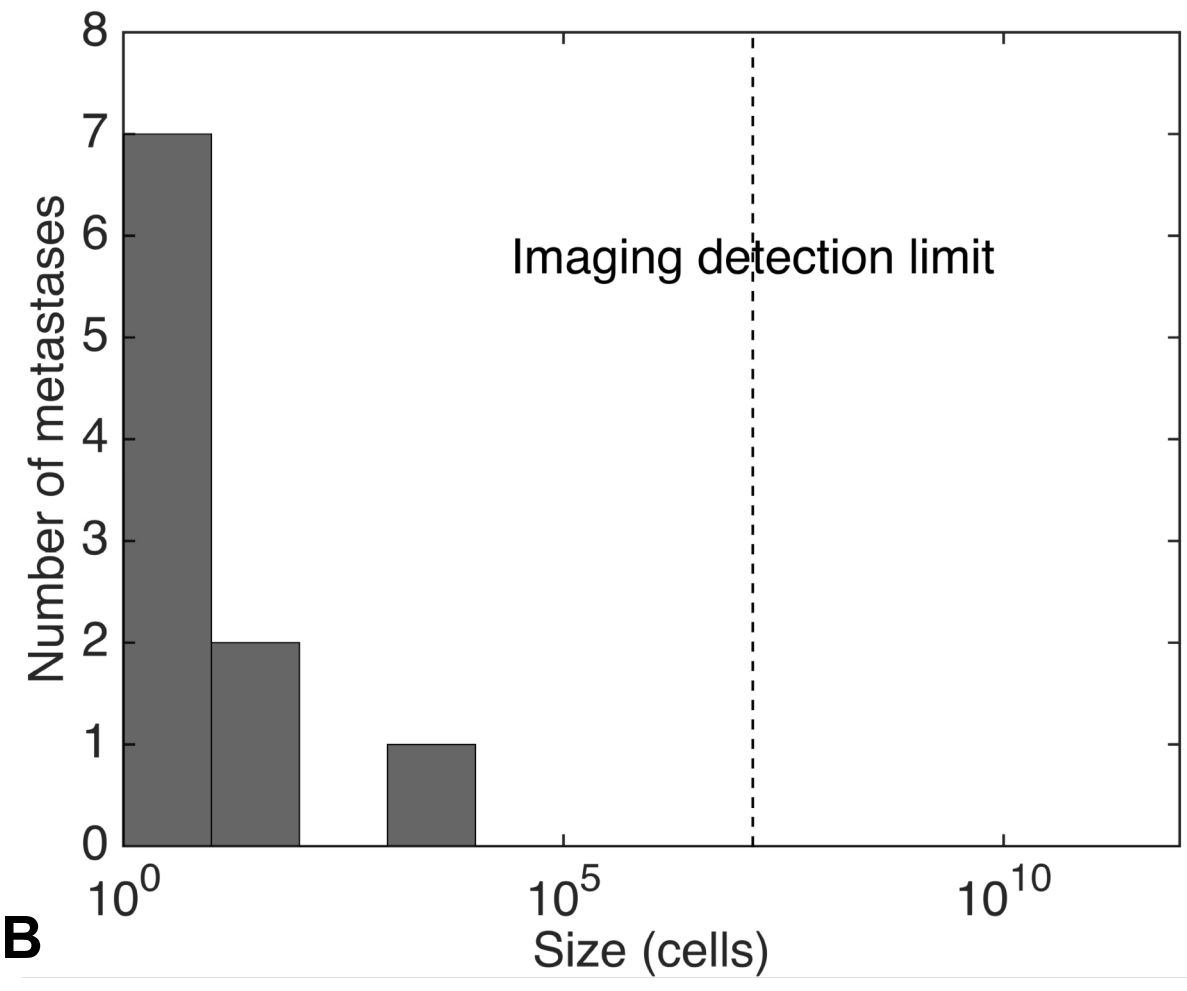
Number of metastases
Imaging detection limit
10^0
10^5
10^{10}
Size (cells)

B

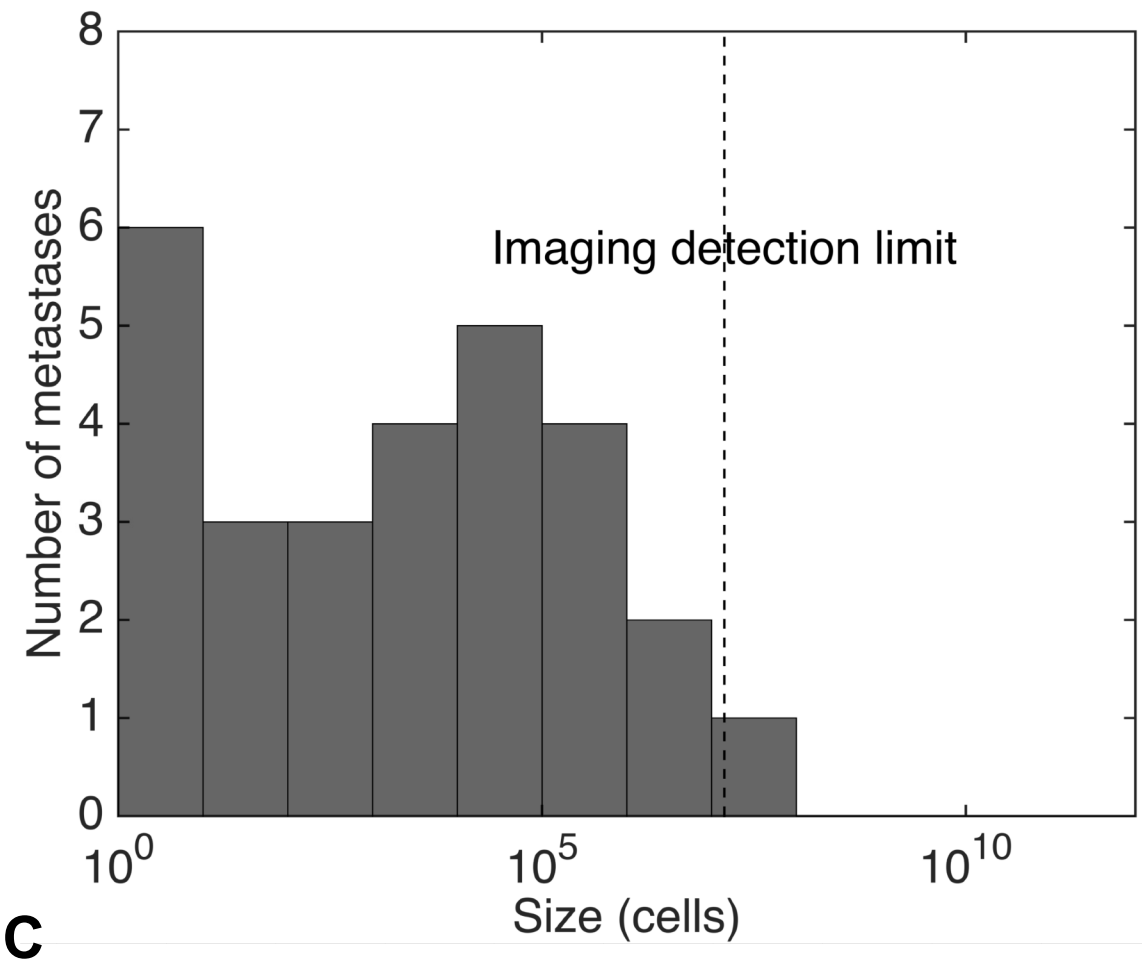
Number of metastases
Imaging detection limit
10^0
10^5
10^{10}
Size (cells)

C